

Available online at www.sciencedirect.com

ScienceDirect

journal homepage: www.ejcancer.com

Original Research

Epigenetic potentiation of somatostatin-2 by guadecitabine in neuroendocrine neoplasias as a novel method to allow delivery of peptide receptor radiotherapy



Joanne S. Evans ^{a,1}, Jamie Beaumont ^{a,1}, Marta Braga ^a, Nahal Masrour ^a, Francesco Mauri ^a, Alice Beckley ^a, Shamus Butt ^a, Christina S. Karali ^a, Chris Cawthorne ^b, Stephen Archibald ^b, Eric O. Aboagye ^a, Rohini Sharma ^{a,*}

^a Department of Surgery and Cancer, Imperial College London, Hammersmith Campus, London, UK

^b Department of Biomedical Sciences, University of Hull, Hull, UK

Received 1 August 2022; accepted 8 September 2022

Available online 5 October 2022

KEYWORDS

Neuroendocrine tumours;
Peptide receptor radionuclide therapy;
SSTR2;
Guadecitabine;
Epigenetic modification

Abstract Background: Somatostatin receptor-2 (SSTR2) is expressed on cell surface of neuroendocrine neoplasias; its presence is exploited for the delivery of peptide receptor radionuclide therapy (PRRT). Patients with no or low expression of SSTR2 are not candidates for PRRT. SSTR2 promoter undergoes epigenetic modification, known to regulate gene expression. We investigated whether the demethylation agent, guadecitabine, could enhance the expression of SSTR2 in NET models, using radioligand uptake/PET imaging as a biomarker of epigenetic modification.

Methods: The effects of guadecitabine on the transcriptional, translational, and functional regulation of SSTR2 both *in vitro* and *in vivo* using low (QGP-1) and high (BON-1) methylated neuroendocrine neoplasia models was characterised. Promotor region methylation profiling of clinical samples (n = 61) was undertaken. Safety of combination guadecitabine and PRRT was assessed *in vivo*.

Results: Pyrosequencing of cell lines illustrated differential methylation indices – BON: 1 94%, QGP: 1 21%. Following guadecitabine treatment, a dose-dependent increase in SSTR2 in BON-1 at a transcriptional, translational, and functional levels using the SSTR2-directed radioligand, ¹⁸F-FET-βAG-TOCA ([¹⁸F]-FETO) (150% increase [¹⁸F]-FETO uptake, p < 0.05) was observed. *In vivo*, guadecitabine treatment resulted in a 70% increase in [¹⁸F]-

* Corresponding author: Imperial Centre for Translational and Experimental Medicine, Department of Surgery and Cancer, Imperial College, Hammersmith Campus, Du Cane Road, London, W12 0NN, Tel.: +44 (0)20 3313 3057.

E-mail address: r.sharma@imperial.ac.uk (R. Sharma).

¹ Denotes joint first authorship.

<https://doi.org/10.1016/j.ejca.2022.09.009>

0959-8049/Crown Copyright © 2022 Published by Elsevier Ltd. This is an open access article under the CC BY license (<http://creativecommons.org/licenses/by/4.0/>).

FETO uptake in BON-1 tumour models compared models with low baseline percentage methylation ($p < 0.05$). No additive toxicity was observed with the combination treatment of PRRT and guadecitabine *in vivo*. Methylation index in clinical samples was 10.5% compared to 5.2% in controls ($p = 0.03$) and correlated with SSTR2 expression (Wilcoxon rank sign $-3.75, p < 0.01$).

Conclusion: Guadecitabine increases SSTR2 expression both *in vitro* and *in vivo*. The combination of demethylation agents with PRRT warrants further investigation.

Crown Copyright © 2022 Published by Elsevier Ltd. This is an open access article under the CC BY license (<http://creativecommons.org/licenses/by/4.0/>).

1. Introduction

Neuroendocrine neoplasias (NENs) are a clinically heterogeneous group of cancers, characterised by the presence of somatostatin receptors (SSTRs) on the tumour surface [1]. The SSTR family comprises of five widely distributed G-protein coupled receptors that mediate intracellular signalling pathways with roles in cell proliferation, cell differentiation and angiogenesis [2]. The expression of the SSTRs on NENs can be exploited for therapeutic benefits with somatostatin analogues (SSAs) and peptide receptor radionuclide therapy (PRRT). Indeed, the long acting SSA preparations octreotide and lanreotide are considered standard of care for the treatment of Grade 1 and 2 NENs within the current European Neuroendocrine Tumour Society Consensus Guidelines, with proven anti-proliferative effects in phase 3 clinical trials [3–5]. The NETTER-1 trial has arguably provided the biggest clinical impact in the treatment of SSTR2-expressing NENs [6]. By comparing ‘double dose’ SSA treatment with PRRT in midgut NET patients progressing on standard dose SSA treatment, the progression-free survival over the first 30 months of the trial for SSA treatment was reported at 8.4 months, with the progression-free survival for ^{177}Lu -DOTATATE not having been reached. This translated to a 79% risk reduction of progression or death for patients treated with PRRT over SSA.

Selection for treatment with PRRT is based on the presence of SSTR2 as illustrated by positive receptor imaging; most frequently using ^{68}Ga -labelled SSAs (^{68}Ga -DOTA-PET) [7]. The only validated predictor of response to PRRT is positive SSTR2 imaging to confirm presence of target, in a binary manner. However, the NETTER1 trial reports an objective response rate for PRRT of 18%, suggesting that a significant number of patients who theoretically should respond do not, and the reasons for this remain unclear [6].

Previous studies have demonstrated that the expression of the SSTR2 receptor is controlled by two epigenetic modifications of a novel SSTR2 upstream promoter: cytosine DNA methylation of key CpG islands and histone acetylation [8]. CpG islands are found most commonly within the regulatory regions of genes: their promoter and 5' coding regions, where

methylation induces transcriptional silencing [8]. This putative upstream promoter area for SSTR2 is conserved across species and is responsible for between 40 and 60% of total SSTR2 production across multiple cell lines representing different cancer types. Methylation of this promoter was demonstrated to be reversible *in vitro* with the first-generation DNA methyltransferase inhibiting agent decitabine [8]. However, decitabine, and its deoxy derivative azacitidine, has limited use in the management of solid tumours due to rapid deamination by cytidine deaminase, limiting tumour drug exposure together with significant dose-limiting myelosuppression [9–11].

The second-generation DNA methyltransferase inhibitor guadecitabine (SGI-110) couples deoxyguanosine to decitabine, thus resistant to cytidine deaminase with a clinically meaningful longer half-life [12]. The described toxicities of myelosuppression and fatigue, and the need for care in renal failure remain similar to those of the first-generation drugs; however, the reduced dosing frequency of guadecitabine may mean that toxicities are encountered less frequently in clinical practice [13,14]. Guadecitabine is currently under evaluation as combination therapy in multiple clinical trials across several different solid tumour types [15–18].

We hypothesised that treatment with a robust DNA methyltransferase inhibitor would increase SSTR2 expression, as visualised by PET imaging. We demonstrate that promoter methylation in SSTR2 can be reversed using guadecitabine resulting in increased uptake of the SSTR2-directed radioligand ^{18}F -FET- β AG-TOCA (^{18}F -FETO) [19] both *in vitro* and *in vivo*, demonstrating for the first time that PET imaging can be used to image epigenetic regulation in NET. We further assessed the safety of combination guadecitabine, and PRRT was assessed *in vivo* and the prevalence of methylation in NENs in clinical samples with a view to moving forward with clinical studies.

2. Materials and methods

2.1. Cell line characteristics and cell culture

All cell lines were obtained from in-house stock and were authenticated (short tandem repeat profiling,

Public Health England); CM cells could not be authenticated as no cell line data were available. Each line was expanded into 10 tubes (1.5×10^6 /mL/tube) and frozen immediately to provide passage calibrated stock for subsequent experiments. QGP1 and CM cells were cultured in Roswell Park Memorial Institute 1640 media. BON-1 cell line was cultured in Dulbecco's modified Eagle's medium. All were supplemented with 10% foetal bovine serum, 2% penicillin-streptomycin (5000 U/mL) and 1% L-glutamine. Cells were seeded at 150,000 cells/mL and grown as a semi-confluent monolayer in a 5% CO₂ humidified incubator at 37 °C. Cells were kept in culture in Falcon flasks for a maximum of 10 passages, before being replaced. Cells were confirmed as *mycoplasma* free every 4 weeks.

2.2. Guadecitabine

Astex Pharmaceuticals (Cambridge, UK) kindly donated guadecitabine. A 16 mM working stock was prepared by dissolving guadecitabine in the provided diluent (Astex Pharmaceuticals) and stored at 4 °C. Cell lines were treated with 0, 5 or 10 μM of guadecitabine, which was replenished, along with fresh media, every 24 h in order to counter against drug inactivation by hydrolysis. Cells were harvested at 72 h and were washed, spun down in to a pellet and stored at −80 °C.

2.3. Tumour tissue

Human tumour tissue from 65 patients was retrieved from the Imperial College Healthcare Tissue Bank (ICHTB). Demographics are shown in Table 1. ICHTB is approved by Wales REC3 to release human material for research (17/WA/0161), and the samples for this project were issued from subcollection reference number R14014.

2.4. DNA extraction

Prior to DNA extraction, optimal tumour slices were selected and deparaffinised. DNA was extracted from human tissue using the QIAamp DNA FFPE Tissue Kit (Qiagen) according to in-house protocols extrapolated

from manufacturer's instructions. DNA was extracted from cell lines using the DNeasy Blood and Tissue Kit (Qiagen), as per manufacturer's instructions. The quality of the extraction was assessed by Nanodrop ND-1000 spectrophotometer (Thermo Scientific), and the amount of DNA extracted was determined using Qubit 2.0 fluorometer (Invitrogen).

2.5. Pyrosequencing of tissue and cell lines

Bisulphite modification of DNA was performed using the EZ DNA Methylation-Lightning™ Kit (Zymo Research Corp), according to manufacturer's instructions. Bisulfite-converted DNA was amplified by methylation-specific PCR (MSP) using SSTR2-specific primers designed and optimised in-house. The resulting amplicon (120 base pairs) included the SSTR2 Transcriptional Start Site and CpG sites of interest as previously described [20]. Pyrosequencing was conducted using Pyromark Q96 (Qiagen), according to manufacturer's instructions. Cell lines and human samples were compared with *in vitro* methylated standards at 25, 50, 75 and 100% to monitor the efficiency of the pyrosequencing reaction, and linear regression analysis applied to generate a standard curve with a correlation coefficient to correct for any assay bias. Human genomic DNA pooled from healthy female and male individuals was used as reference (Promega, G1512 and G1471).

2.6. Cytotoxicity assay

Cells were seeded in a 96-well plate and grown in media with various conditioned media for 72 h. After treatment, 10% trichloroacetic acid was added to the media and the plate incubated at 4 °C for 1 h to fix cells. Plates were washed thoroughly in water and left to dry overnight. Cells were stained in 0.4% SRB dye in 1% acetic acid. Unbound SRB was removed by washing with 1% acetic acid and left overnight; 10 mM Tris was added and optical density measured at 564 nm (Tecan infinite M200). Each unknown optical density value was standardised against the vehicle control.

2.7. qRT-PCR

Total RNA was isolated from cell pellets using the RNeasy Mini Kit (Qiagen), measured by Nanodrop ND-1000 spectrophotometer (Thermo Scientific) and reverse-transcribed using the High-Capacity cDNA Reverse Transcription Kits (Applied Biosystems). Real-time quantitative PCR was conducted using 'TaqMan Fast Advanced Master Mix' (Applied Biosystems) and probes Hs00265624_s1 for SSTR2, Hs02786624_g1 for GAPDH from TaqMan gene expression assays (Applied Biosystems) in a 7900HT Fast Real-Time PCR System (Applied Biosystems). Data were analysed using comparative C_t method as previously described with

Table 1
Characteristics of study population.

Number (%)	65
Site	
Small Bowel	19 (29)
Pancreas	27 (42)
Other	3 (5)
Grade	
1	19 (29)
2	25 (38)
3	2 (3)
Metastatic disease	
No	21 (32)
Yes	48 (74)

GAPDH (Fwd.; Rev.) as an internal control [21]. All samples were assayed in triplicate, with appropriate non-template controls.

2.8. Western blot analysis

Protein samples were prepared by resuspending cell pellets in ice-cold PBS and washing three times. Cell lysis was achieved using ice-cold RIPA buffer (Thermo Scientific). The lysates were sonicated, and protein concentration was determined using the Pierce Detergent Compatible Bradford Assay Kit (Thermo Scientific) and 30 µg of total protein was assayed per sample. Tissue samples were homogenised in RIPA buffer containing protease and phosphatase inhibitors (all Sigma–Aldrich) using a Pre-cellys 24 homogeniser with CK14 beads. Homogenates were cleared of debris by centrifugation at 5000 × g at 4 °C for 5 min. Supernatants were recovered and 30 µg protein assayed. Skimmed dried milk (1% w/v) diluted in TBST solution was used for blocking of non-specific binding sites for 1 h, at room temperature. Membranes were incubated at 4 °C overnight with the anti-SSTR2 primary antibody, SSTR2 (Santa Cruz) (1:1000). After three washings with TBST, the membranes were incubated with a HRP-conjugated secondary antibody. Membranes were incubated with ECL substrate solution (GE Healthcare) according to manufacturer's instructions. β-tubulin and β-actin were used as loading controls.

2.9. Uptake studies

BON-1 cells were grown in six-well plates, seeded at 150,000 cells/well. Guadecitabine was added to the wells at two dilutions (5 and 10 µM) on Day 2, cells replaced with fresh drug containing media every 24 h [¹⁸F]-FETO uptake was conducted 72 h after initiating treatment, by adding the radiotracer in fresh drug-containing medium; each well contained 0.74 MBq of [¹⁸F]-FETO in a volume of 1 ml. Cells were incubated at 37 °C and 5% CO₂ for 1 h and then were washed three times with 1 × PBS and lysed on ice for 15 min using 1 ml RIPA buffer/well. Cell lysates were transferred to respective radioactivity counting tubes. Radioactivity in each sample was counted using an auto gamma counter (Perkin Elmer, London, UK). The amount of protein in each gamma-counted sample was quantified using the Pierce™ BCA protein assay method. Decay-corrected counts were normalised to protein concentration and expressed as percentage incubated dose per milligramme of cellular protein (%ID/mg protein) in each sample.

2.10. PET imaging following guadecitabine treatment and [¹⁸F]FETO uptake

All animal experiments were done by licensed investigators in accordance with the UK Home Office Guidance on the Operation of the Animal (Scientific

Procedures) Act 1986 (HMSO, London, UK, 1990) and within guidelines set out by the UK National Cancer Research Institute Committee on Welfare of Animals in Cancer Research [22].

The *in vivo* models were set up in female athymic nude mice aged 6–8 weeks (Harlan, Bicester, UK Ltd). Xenografts were established under 2.5% isoflurane anaesthesia by subcutaneous injection of either BON-1 or QGP-1 cells on the back of the neck (4 × 10⁶ cells in 100 µL of 50% PBS and 50% Matrigel (Corning, Amsterdam, The Netherlands). Tumour dimensions were measured by calliper and volumes calculated using the ellipsoid formula for estimating tumour mass: volume (mm³) = (π/6) × a × b × c, where a, b and c represent three orthogonal axes of the tumour. When tumours reached 50–70 mm³ (8 weeks post-induction), mice were randomised into vehicle and guadecitabine treatment groups. Guadecitabine was prepared fresh before administration, according to manufacturer's instructions. Guadecitabine-treated mice were injected with 2 mg/kg of the drug subcutaneously twice weekly for 2 weeks; control groups were injected with vehicle (1:50 diluent:PBS) (Supplementary Fig. 1) [23].

For imaging, mice were anesthetized with 2.5% isoflurane and placed in a thermostatically controlled rig in a dedicated small animal Genisys PET scanner (SOFIE Biosciences, Culver City, USA) [24]. Following injection of 0.925 MBq of [¹⁸F]FETO via lateral tail vein cannula, PET scans were acquired in a list-mode format over either 0–60 min after injection to give decay-corrected values of radioactivity accumulation in tissues. The collected data were reconstructed with a three-dimensional maximum likelihood estimation method (3D ML-EM). Volumes of interest for tumours were defined using Siemens Inveon Research Workplace software (Siemens Molecular Imaging Inc., Knoxville, USA) and the count densities (MBq/mL) averaged for the time points corresponding to 3–20 min (where equilibrium was observed). Tissue radioactivity values were normalised to average whole-body radioactivity.

2.11. Combination therapy of guadecitabine and [¹⁷⁷Lu]-DOTATATE *in vivo*

The *in vivo* models were set up in female athymic nude mice aged 6–8 weeks (Harlan, Bicester, UK Ltd). Xenografts were established under 2.5% isoflurane anaesthesia by subcutaneous injection of BON-1 and QGP-1 cell lines (5 × 10⁶ cells in 100 µL of 50% PBS and 50% Matrigel (Corning, Amsterdam, The Netherlands) on the upper flank of the mice. Tumour dimensions were measured by calliper as described above. When tumours reached 200 mm³, mice were randomised into vehicle and guadecitabine treatment groups. Guadecitabine-treated mice were injected with 2 mg/kg of the drug intravenously daily for 5 days; control groups were

injected with normal saline [23]. On Day 7, mice were then randomised to receive either saline or 7.5MBq of [¹⁷⁷Lu]-DOTATATE (six mice in each treatment group) (Supplementary Fig. 1). Tumour growth was assessed by calliper measurements daily. End-point was set to a tumour size of 1000 mm³ or weight loss of more than 10% compared with day of treatment start. Upon reaching end-point, animals were sacrificed and the tumour was collected and snap frozen in liquid nitrogen for further analysis.

3. Histopathology

Formalin-fixed, paraffin-embedded specimens and matching haematoxylin and eosin (H&E) slides were retrieved from the local pathology archive. Five µm thick sections were de-paraffinized in xylene and rehydrated in graded alcohols. Optimal heat-mediated antigen retrieval conditions were applied according to manufacturer's recommendations in relation to the primary antibody, using a water bath heated to 100 °C. Slides were then incubated in citrate buffer at pH 6.0 for 20 min. Before immunostaining, slides were cooled at room temperature, and endogenous peroxidase activity was suppressed by incubation with CAS-Block (Invitrogen, Camarillo, California, USA) for 5 min. The primary antibody against SSTR2A (UMB1, Abcam, Cambridge, UK) was used at a 1:250 dilution overnight. Slides were washed with buffered TRIS solution and blocked with Novolink polymer (Leica, Milton Keynes, UK) for 30 min and subsequently developed with diaminobenzidine and Mayer's Haematoxylin counterstaining. Appropriately, selected tissue sections were used according to the manufacturer's instruction as external positive control during each reaction. Negative control reactions were performed omitting the primary antibodies from the dilution buffer. This resulted in a complete absence of staining in all cases. A trained histopathologist (FM) blinded to the clinical data scored all the cases. Tissue samples were scored manually using the immunohistochemical score (IHS) [25]. Briefly, each sample can be assigned an IHS ranging between 0 and 300, based on the multiplication of the percentage of cells showing immunohistochemical expression (0–100) by the intensity of the signal (graded 1–3).

3.1. Statistical analysis

Quantitative data are presented as mean ± SEM, and $p < 0.05$ was considered significant. Statistical significance for multiple comparisons between control and treated groups was determined by non-parametric one-way ANOVA, while for statistical significance between two groups, Student's t-test was performed. Data analysis was performed by using GraphPad Prism 6.0 or SPSS 23.0 software package (SPSS, Inc., IL, USA).

4. Results

4.1. Methylation status of SSTR2 CpG island in different human NET cell lines

To determine the methylation status of the SSTR2 promoter in the neuroendocrine cell lines BON1, CM and QGP1, we analysed cells using the bisulphite pyrosequencing assay, assessing four CpG islands implicated in SSTR2 epigenetic control [8]. Results showed that the two cell lines derived from NET metastases were heavily methylated: BON1 (methylation index (MI) 94%) and CM (83%), while the non-metastatic line, QGP1 demonstrated the least methylation (21%) (Fig. 1A).

Having demonstrated promoter methylation, we investigated whether this could be modified. Using the novel second-generation DNA-hypomethylating agent, guadecitabine, we assessed methylation reversibility across a range of concentrations, as determined from the cytotoxicity assay performed and informed from published literature (Supplementary Fig. 2A and B) [23,26]. Cells were treated with varying concentrations of guadecitabine, harvested at 72 h and methylation status analysed using pyrosequencing. Statistically significant levels of demethylation were seen at all tested drug concentrations ($p \leq 0.05$), with maximal reversal seen at 10 µM, a finding which was replicated across all three cell lines (Fig. 1A).

4.2. Treatment with guadecitabine results in increased expression of SSTR2 in vitro

Having demonstrated that SSTR2 promoter methylation can be reversed using guadecitabine, we next considered whether this was functionally relevant at the level of mRNA transcription. Treatment with guadecitabine resulted in a significant increase in SSTR2 mRNA in all three cell lines at 72 h, indicating that SSTR2 expression is controlled in an epigenetic manner, and methylation contributes to gene silencing at this locus. Maximal SSTR2 mRNA levels were observed at the 10 µM dose level in all three lines ($p < 0.05$), mirroring the maximal demethylation observed also at this dose (Fig. 1B). Furthermore, we explored the relationship between the methylation state of the SSTR2 upstream promoter and corresponding gene expression. We saw a significant correlation between degree of demethylation and mRNA expression ($R^2 = 0.714$, $p = 0.034$).

We next investigated whether treatment of cell lines with guadecitabine resulted in altered levels of the SSTR2 protein. Cells were treated with guadecitabine at various concentrations (0, 5 and 10 µM), as described, for 72 h. Protein expression was examined by western blot analysis using the SSTR2 primary antibody.

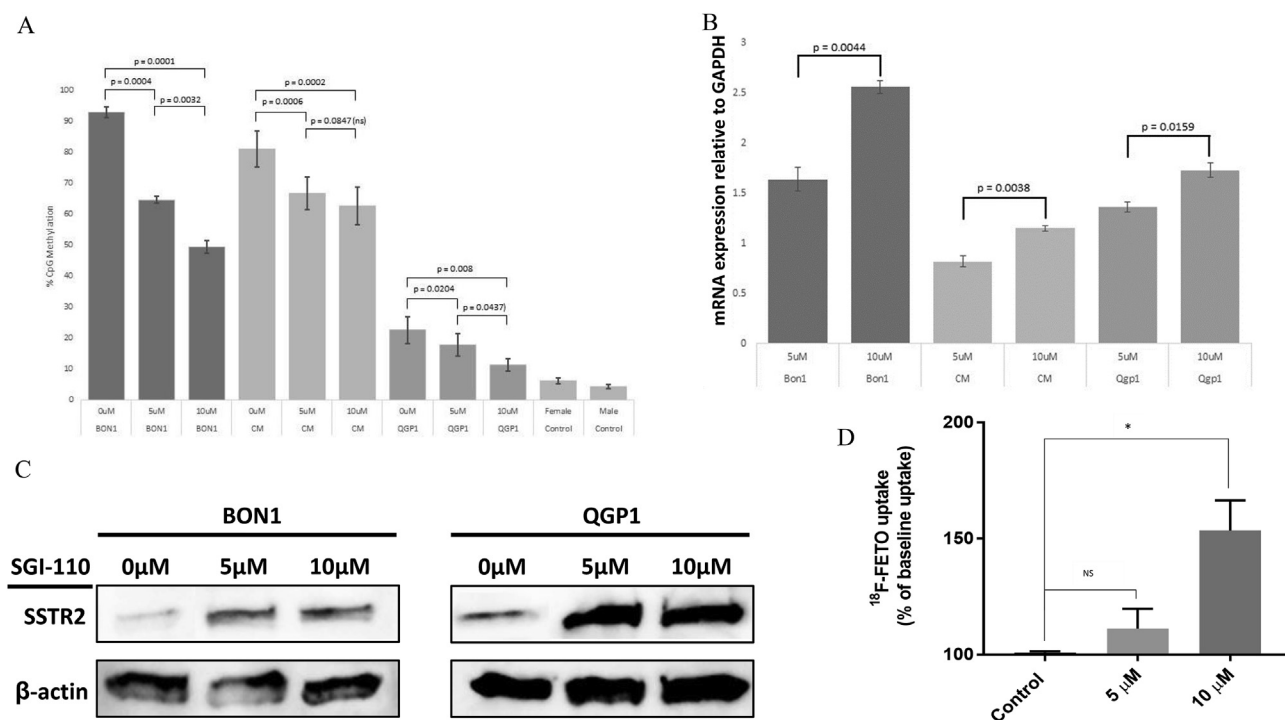


Fig. 1. (A). Bar graph illustrating changes in methylation of SSTR2 promoter region of three NET cell lines: BON-1, CM and QGP-1 following treatment with increasing concentrations of SGI-110 (0, 5 and 10 μM). Cells were treated with SGI-110 for 72 h following which they were harvested, underwent bisulphite conversion followed by pyrosequencing. There was a significant reduction in SSTR2 promoter methylation with increasing concentration of SGI-110 across all three cell lines. Studies in duplicate. Students t-test was used to determine significance. P values are given. (B). Bar graph illustrating the mean relative expression of SSTR2 mRNA in different human neuroendocrine cell lines + SEM. The amount of total SSTR2 mRNA in the indicated cell lines was quantified by q-RT-PCR analysis. GAPDH amplification was used for normalisation. Represented results are expressed as $2^{\text{exp}(-\Delta\text{Ct})}$ using GAPDH as the reference gene. Experiments were performed in triplicate. Students T-Test was used to determine significance. P values are given. (C). Western blots illustrating changes in SSTR2 protein expression with increasing concentrations of SGI-110 (0 μM, 5 μM and 10 μM). β-actin was used as a housekeeper. (D). BON-1 cells were pulsed with [¹⁸F]FETO for 1 h following 72 h treatment with increasing doses of SGI-110 (0 μM, 5 μM, 10 μM) and retained activity measured. Uptake of [¹⁸F]FETO was compared to cells treated with vehicle. Bar graph illustrates percentage of baseline uptake + SEM. One-way ANOVA. P values given above, *p < 0.05, ns – not significant.

Consistent with the result of the RT-PCR, the protein level of SSTR2 was higher following treatment with guadecitabine as compared to untreated cells, in keeping with the observation that demethylation leads to a removal of transcriptional silencing (Fig. 1C).

4.3. SSTR2 is methylated in human NET tissue

DNA methylation in both health and cancer is complex and multifaceted. Although some studies suggest that the methylation status is identical in cell lines and human tissue, this is not supported in other studies; the way in which cell lines are derived, transformed and the expanded lend to the possibility of modifying the epigenetic profile [27,28]. As such, we set out to establish the SSTR2 methylation status in patient samples, and the statistical relationship, if any, to non-NET control tissue. To this end, we extracted DNA from archival tumour material of 80 specimens relating to 65 individual patients and analysed the level of SSTR2 promoter methylation across multiple grades and sites, standardised against methylation controls and compared to non-NET human

tissue. We found a small but statistically significant difference in the methylation index (MI) – at the SSTR2 upstream promoter – between tumour samples and non-NET tissue controls (average MI 10.46 versus 5.22; $p = 0.03$) (Supplementary Fig. 3). Moreover, we report a significant relationship between methylation of the promoter region of SSTR2 and tumour SSTR2 protein expression by IHS (Wilcoxon rank sign -3.75 , $p < 0.01$).

4.4. Increased radioligand uptake with guadecitabine treatment

[¹⁸F]-FETO is a novel fluorinated radioligand with high affinity for SSTR2 as demonstrated by high tumour uptake in patients with a proven-positive [⁶⁸Ga]-DOTA-PET/CT [19,29]. In order to investigate whether demethylation of the SSTR2 promoter yielded functional and targetable SSTR2, we conducted radioligand uptake studies using BON-1 cells cultured with varying concentrations of guadecitabine (0, 5, 10 μM). With increasing dose of guadecitabine, an increase in [¹⁸F]-FETO uptake was observed (Fig. 1D). This

demonstrates that not only does demethylation of the SSTR2 promoter yield increased levels of mRNA and protein but that this increase is function *in vitro*.

4.5. Guadecitabine enables molecular imaging of SSTR2 *in vivo*

We then evaluated whether treatment with guadecitabine would result in enhanced uptake of [¹⁸F]-FETO. Xenografts were established using the highly methylated cell line BON-1 and the low methylated line QGP-1 and treated as described. No change in tumour size was observed following treatment with guadecitabine. At the functional level, treatment with guadecitabine resulted in a 70% increase in [¹⁸F]-FETO in the highly methylated BON-1 model compared to vehicle treatment ($p < 0.001$) (Fig. 2A, Supplementary Fig. 4A–C). No increase in [¹⁸F]-FETO uptake was observed in the QGP-1 mouse model ($p > 0.05$) (Supplementary Fig. 5A–C). The change in receptor expression was confirmed on western blot (Fig. 2B). These results confirm that PET imaging can be used to image changes in receptor expression in response to treatment with a demethylating agent.

4.6. Combination of [¹⁷⁷Lu]-DOTATATE and guadecitabine is safe

The tolerability of a single dose [¹⁷⁷Lu]-DOTATATE with guadecitabine was investigated in a xenograft model with both high (BON-1) and low (QGP-1) methylated cell lines. The dosing schedule was well tolerated as indicated by similar survival between treatment groups (saline–saline 86 days (95%CI: 82.8–89.2), saline-[¹⁷⁷Lu]-DOTATATE 98 days (95%CI: 79.7–116.3), guadecitabine-saline 98 days (95%CI: 80.4–115.6),

guadecitabine-[¹⁷⁷Lu]-DOTATATE 82 days (95%CI: 54.6–109.4)) ($p = 0.2$) (Fig. 3). Moreover, animal weight remained stable across groups (saline–saline median increase 11.3%, saline-[¹⁷⁷Lu]-DOTATATE median increase 7.9%, guadecitabine-saline median increase 14.4%, guadecitabine-[¹⁷⁷Lu]-DOTATATE median increase 3.0%) ($p < 0.2$). Animal health was also similar between treatment groups with no acute toxicities noted.

Interestingly, neither single-agent guadecitabine, single-agent [¹⁷⁷Lu]-DOTATATE or combination therapy had an impact on tumour size at the doses studied (Supplementary Fig. 6).

5. Discussion

PRRT treatment represents the only biomarker driven treatment for NENs, with treatment targeted to SSTR2 expression as determined by [⁶⁸Ga]-DOTA imaging [6]. Emerging data suggest that qualitative-positive [⁶⁸Ga]-DOTA imaging *per se* does not accurately predict outcome to PRRT but that semi-quantitative tumour SUV measure is a better predictor of therapeutic outcome, whereby patients with low [⁶⁸Ga]-DOTA SUV have poor outcomes compared to those with higher uptake [30,31]. Moreover, some patients will have negative SSTR2-specific imaging making them unsuitable for therapy [6]. Transient enhancement of SSTR2 expression in patients with negative [⁶⁸Ga]-DOTA imaging may represent a novel method by which the number of patients that receive and respond to PRRT could be increased. We confirm that the SSTR2 gene expression is controlled by methylation-specific gene silencing via an upstream promoter, as previously demonstrated [8]. We add to this mechanistically relevant information by revealing that promoter methylation can be transiently reversed by the demethylating agent guadecitabine in a

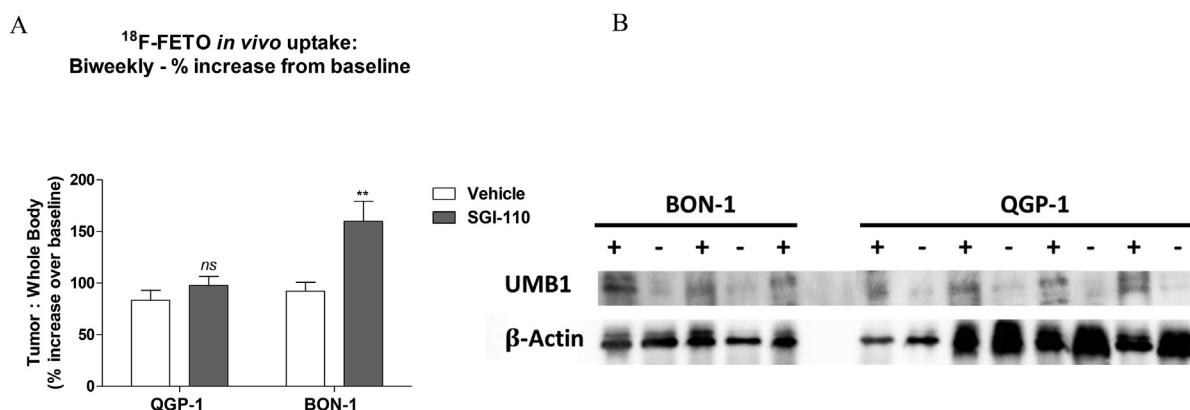


Fig. 2. Uptake of 18 F-FETO in tumours following guadecitabine treatment. Tumour-to-whole body ratios were derived from region-of-interest analysis of the summed PET images over a period of 3–20 min after intravenous injection of 1.48 MBq of 18 F-FETO in mice treated every 3 days with 2 mg/kg guadecitabine or vehicle (50:1 PBS:diluent) by subcutaneous injection over a period of 10 days (A) Data are expressed as % of change between baseline scan (day 0) and post-treatment scan (day 10). (B) Western blot confirmed an increase in SSTR2 protein expression using UMB1 relative to β-actin within tumour tissue samples from mice. “+” illustrates treatment with guadecitabine and “-” illustrates vehicle treatment. Students T-Test was used to determine significance. ** $p < 0.01$, ns – not significant.

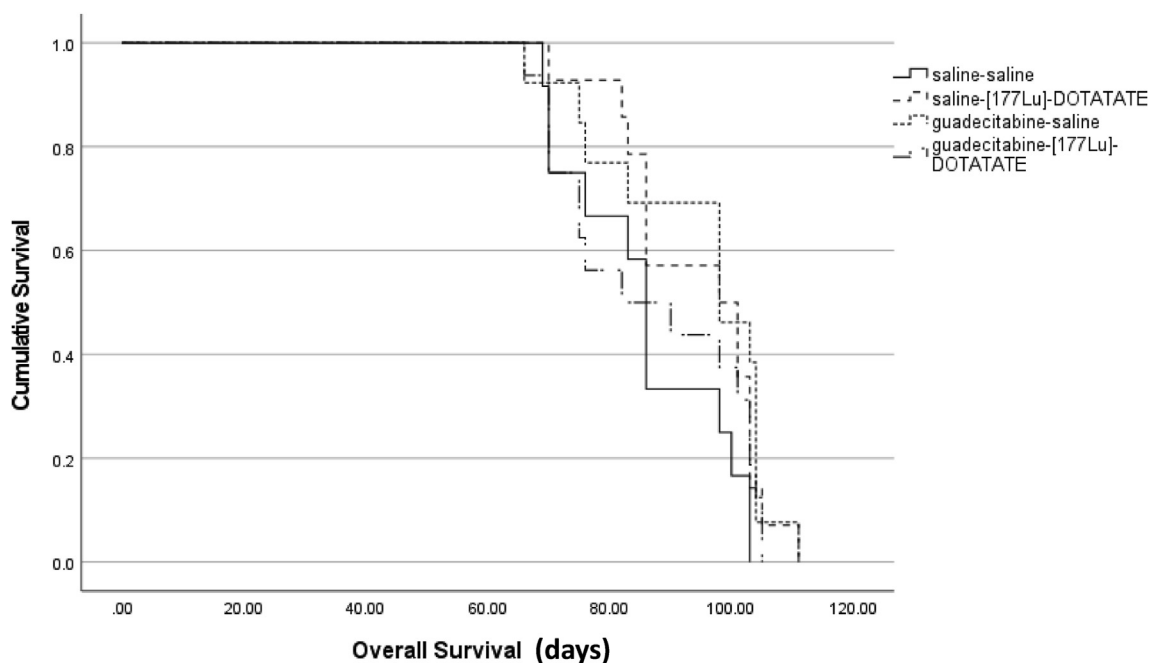


Fig. 3. Kaplan–Meier survival curves where survival end-point was defined as the time the tumour volume reached 1000 mm³ or weight loss of more than 10% compared with day of treatment start.

drug concentration related manner, leading to both increased transcription and translation of the SSTR2 gene product. Crucially, we illustrate that the upregulation of SSTR2 is detectable by PET imaging, thus illustrating for the first time that PET imaging can be used to monitor the epigenetic change.

In the largest published patient cohort to date, we report the MI of the SSTR2 upstream promotor in 65 tumour samples, compared to non-NET standardised controls, revealing a statistically significant difference in MI that correlated inversely with SSTR2 expression. Several studies have illustrated that SUV is correlated with SSTR2 tissue expression and is predictive of outcome to PRRT [30–34]. Taken together with the findings in this study, it can be hypothesised that methylation of SSTR2 does not result in complete epigenetic silencing of the receptor but a reduction in expression which can be enhanced using a DNA hypomethylating agent to improve the efficacy of PRRT.

While previous studies investigated the use of decitabine, this drug has limited use in the management of solid tumours due to rapid deamination by cytidine deaminase limiting tumour drug exposure, and significant dose-limiting myelosuppression. Guadecitabine is a novel second generation hypomethylating agent, made of the active moiety of decitabine and deoxyguanosine linked by a phosphodiester bond. The phosphodiester bond undergoes gradual cleavage by phosphorylases and other enzymes over an extended period of time, prolonging drug exposure [23]. Guadecitabine has a half-life of 4 h in humans compared to decitabine that has a half-life of 30 min [26]. Moreover, guadecitabine is resistant to

cytidine deaminase resulting in improved tumour drug exposure. In clinical studies, guadecitabine had a lower C_{max} compared to decitabine resulting in less toxicity, in particular myelosuppression, a key dose-limiting side-effect that limits the use of decitabine [26,35–37]. Consistent with previous findings using decitabine, we illustrated that treatment of NET cell lines with the demethylating agent, guadecitabine, not only resulted in re-expression of SSTR2 but importantly resulted in enhanced uptake of [¹⁸F]-FETO [38,39]. [¹⁸F]-FETO, a [¹⁸F]labelled octreotate, was developed by our group to obviate the need for an on-site gallium generator – due to the short half-life of [⁶⁸Ga] [29]. [¹⁸F]-FETO has recently been shown to result in clinical quality images and was therefore taken forward in this study with a view to taking this tracer forward in the clinical setting [19].

We extended our *in vitro* findings into a mouse model of NET using BON-1 cells (high methylation and low basal expression SSTR2) and QGP-1 (low methylation and high basal expression SSTR2). At the guadecitabine doses studied, we did not observe any change in tumour size. However, the dose administered was sufficient to significantly increase SSTR2 expression within the tumour as reflected by an increased in [¹⁸F]-FETO uptake, rendering undetectable BON-1 xenografts into clearly detectable tumours. In addition we conducted a *in vivo* tolerability study using a single dose of [¹⁷⁷Lu]-DOTATATE in tumour models from the cell lines studied *in vitro*. We did not observe any additive toxicity when guadecitabine was combined with [¹⁷⁷Lu]-DOTATATE a key consideration as both drugs are associated with myelotoxicity. Changes in

tumour size were not observed with combination therapy. While these observations somehow challenges the downstream consequences of our hypothesis of reversing SSTR2 silencing, we also observed slow tumour growth of the NEN models studied, such that a single dose of [¹⁷⁷Lu]-DOTATATE was unlikely to induce changes in tumour size within the bounds of the study including consideration of animal welfare. Future work should consider either multiple dosing experiments or models with more robust growth, considering differential methylation states. Moreover [¹⁷⁷Lu]-DOTATATE was administered when tumour size was relatively large which may have impacted on tumour response. [¹⁷⁷Lu] is a short-range particle, tissue penetration 1.4 mm, and tumour size has a significant impact on the biodistribution of [¹⁷⁷Lu] [40]. Further optimisation of regimen is required to show a reduction in tumour size.

Taken together, this work suggests SSTR2 epigenetic silencing can be reversed, enabling future optimisation of therapeutic options in patients with negative [⁶⁸Ga]-DOTA-PET scans or marginal expression of SSTR2, not suitable for PRRT, using [¹⁸F]-FETO- or other SSA-PET imaging procedure as a measure of epigenetic change. As such, we postulate that producing an increased density of functional SSTR2 will (i) augment response in patients with low [⁶⁸Ga]-DOTA uptake and (ii) transiently upregulate SSTR2 expression in patients with negative functional imaging such that they can receive PRRT. While this concept has not been assessed clinically, Taelman and colleagues illustrated enhanced cell death with [¹⁷⁷Lu]-DOTATATE following treatment with epigenetic modifiers using a number of other cell lines [39]. The authors also illustrated that inhibitors of histone deacetylation (HDAC) upregulated SSTR expression albeit to a lesser degree. It would be of interest to investigate novel HDAC agents in future combination studies using different *in vivo* models to allow maximal re-expression of SSTR2 prior to clinical translational. Any proposed clinical study would have to have clear safety end-points particularly given the potential for additive myelotoxicity and renal toxicity with [¹⁷⁷Lu]-DOTATATE and demethylating agents. While we did not observe additive toxicity *in vivo*, only a single dose of [¹⁷⁷Lu]-DOTATATE was administered and repeat dosing experiments should be undertaken *in vivo* with relevant safety end-points evaluated prior to clinical translation.

While we have illustrated SSTR2 expression can be modulated using demethylating agents in NENs, this is not limited to this tumour type. Previous work illustrates that SSTR is present in a number of different tumour types [41], and there is growing interest in pursuing PRRT for these tumour types. The role of methylation remains to be elucidated but the combination of a demethylation agent and PRRT could potentially be extended to other cancer types.

6. Conclusion

In this study, we demonstrate that the methylation index of the upstream promoter of SSTR2 is significantly higher in NET tissue compared with non-tumour control in patient samples. We showed that epigenetic modification of SSTR2 in key NET cell lines with the demethylating agent guadecitabine can transiently reverse methylation at SSTR2, which in turn leads to functional upregulation of receptor. This may be of benefit in exploring the application for demethylating agents in improving outcomes to targeted treatments, including PRRT in NENs. This approach warrants further evaluation.

Authors contribution

Joanne S. Evans: Data curation; Formal analysis; Investigation; Methodology; Project administration; Supervision; Validation; Visualization; Roles/Writing – original draft.

Jamie Beaumont: Data curation; Formal analysis; Investigation; Methodology; Roles/Writing – original draft.

Marta Braga: Data curation; Formal analysis; Investigation; Methodology; Roles/Writing – original draft.

Nahal Masrou: Data curation; Formal analysis; Investigation; Methodology; Roles/Writing – original draft.

Francesco Mauri: Data curation; Formal analysis; Investigation; Methodology; Roles/Writing – original draft.

Alice Beckley: Data curation; Formal analysis; Investigation; Methodology; Roles/Writing – original draft.

Shamus Butt: Data curation; Formal analysis; Investigation; Methodology; Roles/Writing – original draft.

Christina Simoglou Karali: Data curation; Formal analysis; Investigation; Methodology; Roles/Writing – original draft.

Chris Cawthorne: Conceptualization; Data curation; Formal analysis; Funding acquisition; Investigation; Methodology; Roles/Writing – original draft.

Stephen Archibald: Conceptualization; Data curation; Formal analysis; Funding acquisition; Investigation; Methodology; Roles/Writing – original draft.

Eric O. Aboagye: Conceptualization; Data curation; Formal analysis; Funding acquisition; Investigation; Methodology; Project administration; Resources; Software; Writing – review & editing.

Rohini Sharma: Conceptualization; Data curation; Formal analysis; Funding acquisition; Investigation; Methodology; Project administration; Resources; Software; Supervision; Validation; Visualization; Roles/Writing – original draft; Writing – review & editing.

Funding

Infrastructure support was provided by the National Institute for Health Research (NIHR) Imperial Biomedical Research Centre (BRC) in the form of resource support. Funding from Cancer Research UK (A24604).

Conflict of interest statement

The authors declare the following financial interests/personal relationships which may be considered as potential competing interests: RS: Astex pharmaceuticals, MSD, Bayer, Incyte pharmaceuticals, AAA, Boston Scientific, SIRTEX

No other authors have any interests to declare.

Acknowledgement

Tissue samples were provided by the Imperial College Healthcare NHS Trust Tissue Bank funded by the National Institute for Health Research (NIHR) Biomedical Research Centre based at Imperial College Healthcare NHS Trust and Imperial College London. EOA acknowledges support from Medical Research Council (MC-A652-5PY80) and Imperial Experimental Cancer Medicines Centre. The views expressed are those of the author(s) and not necessarily those of the NHS, the NIHR or the Department of Health.

Appendix A. Supplementary data

Supplementary data to this article can be found online at <https://doi.org/10.1016/j.ejca.2022.09.009>.

References

- [1] Kloppel G. Tumour biology and histopathology of neuroendocrine tumours. *Best Pract Res Clin Endocrinol Metabol* 2007;21:15–31.
- [2] Volante M, Bozzalla-Cassione F, Papotti M. Somatostatin receptors and their interest in diagnostic pathology. *Endocr Pathol* 2004;15:275–91.
- [3] Pavel M, O'Toole D, Costa F, et al. ENETS Consensus guidelines update for the management of distant metastatic disease of intestinal, pancreatic, bronchial neuroendocrine neoplasms (NEN) and NEN of unknown primary site. *Neuroendocrinology* 2016;103:172–85.
- [4] Rinke A, Müller HH, Schade-Brittinger C, et al. Placebo-controlled, double-blind, prospective, randomized study on the effect of octreotide LAR in the control of tumor growth in patients with metastatic neuroendocrine midgut tumors: a report from the PROMID study group. *J Clin Oncol* 2009;27(28):4656–63. <https://doi.org/10.1200/JCO.2009.22.8510>.
- [5] Caplin ME, Pavel M, Ruzniewski P. Lanreotide in metastatic enteropancreatic neuroendocrine tumors. *N Engl J Med* 2014;371:1556–7.
- [6] Strosberg J, Krenning E. 177Lu-Dotatate for midgut neuroendocrine tumors. *N Engl J Med* 2017;376:1391–2.
- [7] Sanli Y, Garg I, Kandathil A, et al. Neuroendocrine tumor diagnosis and management: (68)Ga-dotatate PET/CT. *AJR Am J Roentgenol* 2018;211:267–77.
- [8] Torrisani J, Hanoun N, Laurell H, et al. Identification of an upstream promoter of the human somatostatin receptor, hSSTR2, which is controlled by epigenetic modifications. *Endocrinology* 2008;149:3137–47.
- [9] Fenaux P, Mufti GJ, Hellstrom-Lindberg E, et al. Azacitidine prolongs overall survival and reduces infections and hospitalizations in patients with WHO-defined acute myeloid leukaemia compared with conventional care regimens: an update. *Ecancer-medicalscience* 2008;2:121.
- [10] Kaminskas E, Farrell AT, Wang YC, et al. FDA drug approval summary: azacitidine (5-azacytidine, Vidaza) for injectable suspension. *Oncol* 2005;10:176–82.
- [11] Momparler RL, Goodman J. In vitro cytotoxic and biochemical effects of 5-aza-2'-deoxycytidine. *Cancer Res* 1977;37:1636–9.
- [12] Rogstad DK, Herring JL, Theruvathu JA, et al. Chemical decomposition of 5-aza-2'-deoxycytidine (Decitabine): kinetic analyses and identification of products by NMR, HPLC, and mass spectrometry. *Chem Res Toxicol* 2009;22:1194–204.
- [13] Yoo CB, Jeong S, Egger G, et al. Delivery of 5-aza-2'-deoxycytidine to cells using oligodeoxynucleotides. *Cancer Res* 2007;67:6400–8.
- [14] Derissen EJ, Beijnen JH, Schellens JH. Concise drug review: azacitidine and decitabine. *Oncol* 2013;18:619–24.
- [15] Oza AM, Matulonis UA, Alvarez Secord A, et al. A randomized phase II trial of epigenetic priming with guadecitabine and carboplatin in platinum-resistant, recurrent ovarian cancer. *Clin Cancer Res* 2020;26:1009–16.
- [16] Matei D, Ghamande S, Roman L, et al. A phase I clinical trial of guadecitabine and carboplatin in platinum-resistant, recurrent ovarian cancer: clinical, pharmacokinetic, and pharmacodynamic analyses. *Clin Cancer Res* 2018;24:2285–93.
- [17] Di Giacomo AM, Covre A, Finotello F, et al. Guadecitabine plus ipilimumab in unresectable melanoma: the NIBIT-M4 clinical trial. *Clin Cancer Res* 2019;25:7351–62.
- [18] Lee V, Wang J, Zahurak M, et al. A phase I trial of a guadecitabine (SGI-110) and irinotecan in metastatic colorectal cancer patients previously exposed to irinotecan. *Clin Cancer Res* 2018;24:6160–7.
- [19] Dubash SR, Keat N, Mapelli P, et al. Clinical translation of a click-labeled 18F-octreotate radioligand for imaging neuroendocrine tumors. *J Nucl Med* 2016;57:1207–13.
- [20] Torrisani J, Hanoun N, Laurell H, et al: Identification of an upstream promoter of the human somatostatin receptor, hSSTR2, which is controlled by epigenetic modifications. [academic.oup.com].
- [21] Schmittgen TD, Livak KJ. Analyzing real-time PCR data by the comparative C(T) method. *Nat Protoc* 2008;3:1101–8.
- [22] Workman P, Aboagye EO, Balkwill F, et al. Guidelines for the welfare and use of animals in cancer research. *Br J Cancer* 2010;102:1555–77.
- [23] Fang F, Munck J, Tang J, et al. The novel, small-molecule DNA methylation inhibitor SGI-110 as an ovarian cancer chemosensitizer. *Clin Cancer Res* 2014;20:6504–16.
- [24] Witney TH, Pisaneschi F, Alam IS, et al. Preclinical evaluation of 3-18F-fluoro-2,2-dimethylpropionic acid as an imaging agent for tumor detection. *J Nucl Med* 2014;55:1506–12.
- [25] Pinato DJ, Tan TM, Toussi ST, et al. An expression signature of the angiogenic response in gastrointestinal neuroendocrine tumours: correlation with tumour phenotype and survival outcomes. *Br J Cancer* 2014;110:115–22.
- [26] Issa JJ, Roboz G, Rizzieri D, et al. Safety and tolerability of guadecitabine (SGI-110) in patients with myelodysplastic syndrome and acute myeloid leukaemia: a multicentre, randomised, dose-escalation phase 1 study. *Lancet Oncol* 2015;16:1099–110.
- [27] Varley KE, Gertz J, Bowling KM, et al. Dynamic DNA methylation across diverse human cell lines and tissues. *Genome Res* 2013;23:555–67.

- [28] Ueki T, Walter KM, Skinner H, et al. Aberrant CpG island methylation in cancer cell lines arises in the primary cancers from which they were derived. *Oncogene* 2002;21:2114–7.
- [29] Leyton J, Iddon L, Perumal M, et al. Targeting somatostatin receptors: preclinical evaluation of novel 18F-fluoroethyltriazole-Tyr3-octreotate analogs for PET. *J Nucl Med* 2011;52:1441–8.
- [30] Sharma R, Wang WM, Yusuf S, et al. 68Ga-DOTATATE PET/CT parameters predict response to peptide receptor radionuclide therapy in neuroendocrine tumours. *Radiother Oncol* 2019;141:108–15.
- [31] Haug AR, Auernhammer CJ, Wangler B, et al. 68Ga-DOTA-TATE PET/CT for the early prediction of response to somatostatin receptor-mediated radionuclide therapy in patients with well-differentiated neuroendocrine tumors. *J Nucl Med* 2010;51:1349–56.
- [32] Kratochwil C, Stefanova M, Mavriopoulou E, et al. SUV of [68Ga]DOTATOC-PET/CT predicts response probability of PRRT in neuroendocrine tumors. *Mol Imag Biol* 2015;17:313–8.
- [33] Brunner P, Jorg AC, Glatz K, et al. The prognostic and predictive value of sstr2-immunohistochemistry and sstr2-targeted imaging in neuroendocrine tumors. *Eur J Nucl Med Mol Imag* 2017;44:468–75.
- [34] Kaemmerer D, Prasad V, Daffner W, et al. Neoadjuvant peptide receptor radionuclide therapy for an inoperable neuroendocrine pancreatic tumor. *World J Gastroenterol* 2009;15:5867–70.
- [35] Pleyer L, Greil R. Digging deep into “dirty” drugs - modulation of the methylation machinery. *Drug Metab Rev* 2015;47:252–79.
- [36] Schrupp DS, Fischette MR, Nguyen DM, et al. Phase I study of decitabine-mediated gene expression in patients with cancers involving the lungs, esophagus, or pleura. *Clin Cancer Res* 2006;12:5777–85.
- [37] Stewart DJ, Issa JP, Kurzrock R, et al. Decitabine effect on tumor global DNA methylation and other parameters in a phase I trial in refractory solid tumors and lymphomas. *Clin Cancer Res* 2009;15:3881–8.
- [38] Veenstra MJ, van Koetsveld PM, Dogan F, et al. Epidrug-induced upregulation of functional somatostatin type 2 receptors in human pancreatic neuroendocrine tumor cells. *Oncotarget* 2018;9:14791–802.
- [39] Taelman VF, Radojewski P, Marincek N, et al. Upregulation of key molecules for targeted imaging and therapy. *J Nucl Med* 2016.
- [40] de Jong M, Breeman WA, Valkema R, et al. Combination radionuclide therapy using 177Lu- and 90Y-labeled somatostatin analogs. *J Nucl Med* 2005;46(Suppl 1):13S–7S.
- [41] Taelman VF, Radojewski P, Marincek N, et al. Upregulation of key molecules for targeted imaging and therapy. *J Nucl Med* 2016;57:1805–10.